

# Preparation of transparent oxyapatite ceramics by combined use of freeze-drying and spark-plasma sintering

A. Chesnaud,<sup>a</sup> C. Bogicevic,<sup>a</sup> F. Karolak,<sup>a</sup> C. Estournès<sup>b</sup> and G. Dezanneau<sup>\*a</sup>

Received (in Cambridge, UK) 29th November 2006, Accepted 15th January 2007

First published as an Advance Article on the web 30th January 2007

DOI: 10.1039/b615524c

Lanthanum silicate oxyapatites, ion-conducting materials presenting a strong aversion against densification, have been obtained in the form of dense transparent ceramics, by combining the beneficial use of freeze-drying and spark plasma sintering methods.

Lanthanum silicate oxyapatite compounds have been presented recently as promising electrolyte materials in solid oxide fuel cells, due to their high level of oxygen conduction (and poor electronic conduction) in both oxygen-rich and oxygen-poor atmospheres,<sup>1,2</sup> even in Fe-doped samples.<sup>3</sup> A detailed study on the influence of different lanthanides and of doping on conduction properties can be found in ref. 4. The main limitation of such materials resides in the difficulty to prepare dense ceramics, which is necessary for the envisaged application. For instance, solid state reactions methods at very high temperature (1700 °C during 2 h) leads to a moderately good density of 87%<sup>5</sup> and the use of lower temperatures such as 1500 °C during 16 h lead to poorly densified samples with relative density lower than 70%.<sup>6</sup> Even the use of soft chemistry hardly leads to totally convincing results. Sol-gel methods lead only to relative densities smaller than 80% even after sintering of 1400 °C during 3 days or 1500 °C during 22 h.<sup>7</sup> Recent research gives significantly better results with a density of 92% after 1400 °C/2 h but implies an additional milling step.<sup>8</sup> Here, we present the combined use of a freeze-drying and spark plasma sintering process for the preparation of fully dense and transparent lanthanum silicate oxyapatite ceramics. These results are obviously interesting for the SOFCs community but may also interest those working on luminescent/optical applications based on rare-earth silicon apatites.<sup>9,10</sup>

First, lanthanum silicate nanopowders with composition  $\text{La}_{9,33}\text{Si}_6\text{O}_{26}$  were prepared by freeze-drying. Commercial reagents such as lanthanum acetate,  $\text{La}(\text{CH}_3\text{COO})_3 \cdot 1.5\text{H}_2\text{O}$  (Alfa Aesar, 99.9%) and tetraethoxysilane,  $\text{Si}(\text{OC}_2\text{H}_5)_4$  (TEOS, Strem chemicals, min. 98%) were used as  $\text{La}^{3+}$  and  $\text{Si}^{4+}$  precursors. To obtain ~10 g of apatite materials, a solution with a concentration of 0.01 M of product was prepared. First, according to the composition, 16.006 g of lanthanum acetate was completely dissolved in ultra-pure water. In another beaker, ~6.7 ml of TEOS and ~27 mL of acetic acid (AA) were mixed to give a clear transparent solution that remained

unchanged upon storage under room conditions. Acetic acid is a double agent used to catalyze and to control the hydrolysis reaction of TEOS reactant. For the synthesis, the volumetric ratio,  $r = V_{\text{AA}}/V_{\text{TEOS}}$  was set to 4. Then, the two above-mentioned solutions were mixed and no turbidity or precipitate was observed at this stage: the total volume of the resulting clear transparent solution obtained was 600 ml and the pH value was near 3.8. A vigorous stirring was maintained during 30 min to ensure good homogeneity. The resultant solution was sprayed into liquid nitrogen to form frozen droplets of the solution. Since these micro-droplets were instantaneously flash frozen, the homogeneity of the original solution was retained. These frozen droplets were transferred into the chamber of the freeze-dryer, under vacuum, as quickly as possible. The freeze-drying process was carried out, in a Christ Alpha 2–4 L.S.C. apparatus, for 24 h under  $7.5 \times 10^{-6}$  Torr (1 Torr =  $10^{-5}$  bar), with the temperature of the condenser fixed at 230 K. As the sublimation of the frozen solution occurs, the temperature of the precursor increases progressively up to +10 °C. Then, the temperature was progressively increased to 50 °C while maintaining vacuum. When no variation of the pressure in the chamber was recorded, the freeze-drying process was considered successful. The obtained precursor was then calcined at 1000 °C/4 h. Actually, a temperature of 900 °C is sufficient to obtain well crystallised powder without any parasitic phase.

To perform the sintering step, a quantity of powder was introduced in a graphite piston-cylinder ensemble to form a final pellet 1 mm thick and of 8 mm in diameter. The spark plasma sintering apparatus is a Dr Sinter 2080 set-up as available at the Plateforme Nationale de Frittage Flash at Toulouse (France). Two sintering temperatures (1200 and 1500 °C) were used with different thermal cycles. In both cases, the temperature was increased up to 600 °C at a rate of 300 °C  $\text{min}^{-1}$  and maintained during 1 min while pressure (100 MPa) was applied. After this first step, the temperature was increased with a rate of 50 °C  $\text{min}^{-1}$  to the desired value (1200 or 1500 °C). For the 1200 °C sintering, the pressure and maximum temperature was applied during 3 min and then the pressure and heating power was quickly released. For the 1500 °C sintering temperature, the pressure and power were released when the desired temperature was reached. Natural cooling of the system takes around 10 min. The whole sintering process from sample preparation until final cooling lasts less than 1 h. Samples were then heat-treated in air during 12 h at 1000 °C. This thermal treatment has been chosen to burn all residual carbon species. It has not been optimised and can probably be shortened and lowered in temperature.

The morphology of the powder after calcination is shown on Fig. 1 for different scales. It consists of soft agglomerates with

<sup>a</sup>Laboratoire Structures, Propriétés et Modélisation des Solides, Grande voie des vignes, Ecole Centrale Paris, F-92295, Châtenay-Malabry Cedex, France. E-mail: guilhem.dezanneau@ecp.fr; Fax: +33 1 41131437; Tel: +33 1 41131420

<sup>b</sup>Plateforme Nationale de Frittage Flash, PNF 2 – MHT – UPS, CIRIMAT UMR5085 CNRS/UPS/INP, 118 Route de Narbonne, 31062, Toulouse, France. E-mail: estourne@chimie.ups-tlse.fr; Fax: +33 561557476; Tel: 33 561557475

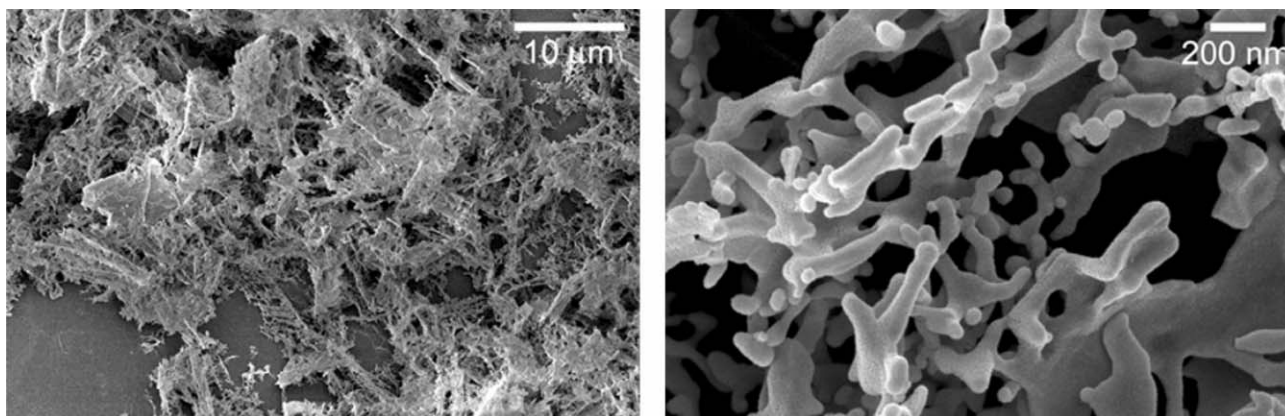


**Fig. 1** Morphology at different scales of the  $\text{La}_{0.33}\text{Si}_6\text{O}_{26}$  nanopowders as obtained after calcination.

submicronic size. Contrarily to classical sol-gel methods, the particles are not strongly agglomerated which may explain in part the enhanced densification explained below. The smaller native particles have a size of smaller than 100 nm. The coherent crystallite size as determined from the Scherrer law applied on (1, 0, 2) and (2, 1, 0) reflections is 54(1) nm, confirming the nanometric nature of the powder.

Fig. 2 shows the X-ray diffraction diagram of the initial raw powders of both samples sintered by SPS. All peaks can be indexed in an hexagonal apatite phase as shown by comparison with the simulated diagram taken from previously published structural data.<sup>11,12</sup>

Images of the obtained ceramics after polishing are shown in Fig. 3. This figure shows that the obtained samples present a vitreous aspect and are transparent, which indicates an almost 100% relative density. Actually, the relative density as measured from weight to volume ratio is also 100% for both samples, within the relative precision of measurements (evaluated at 0.5%). Fig. 4 shows scanning electron microscope (SEM) images of both sintered samples revealing the very high density of the samples with no porosity evident. Nevertheless, a strong difference in grain sizes is observed between both sintered samples. Indeed, the

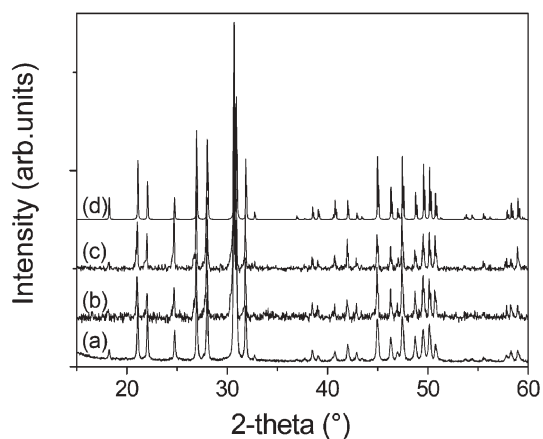


**Fig. 2** X-Ray diffraction patterns of  $\text{La}_{0.33}\text{Si}_6\text{O}_{26}$ . (a) Nanopowder calcined at 1000 °C/4 h; (b) sample sintered by SPS at 1200 °C/3 min; (c) sample sintered by SPS at 1500 °C/18 min; and (d) theoretical diagram as calculated from ref. 11.

sample sintered at 1200 °C during 3 min presents grain sizes in the range 100–500 nm while the sample sintered at 1500 °C presents grain sizes greater than 1 μm and most often in the range 3–5 μm. This confirms that this method allows controlling the microstructure of the sample maintaining a high level of densification. It is now well-known that spark plasma sintering is a powerful method to obtain full density ceramic samples. We are nevertheless convinced that the initial powder has also a strong importance and the main point is probably that the powder has a low level of particle aggregation. This can be achieved easily by freeze-drying and surely other soft chemistry methods can be employed.<sup>15</sup>

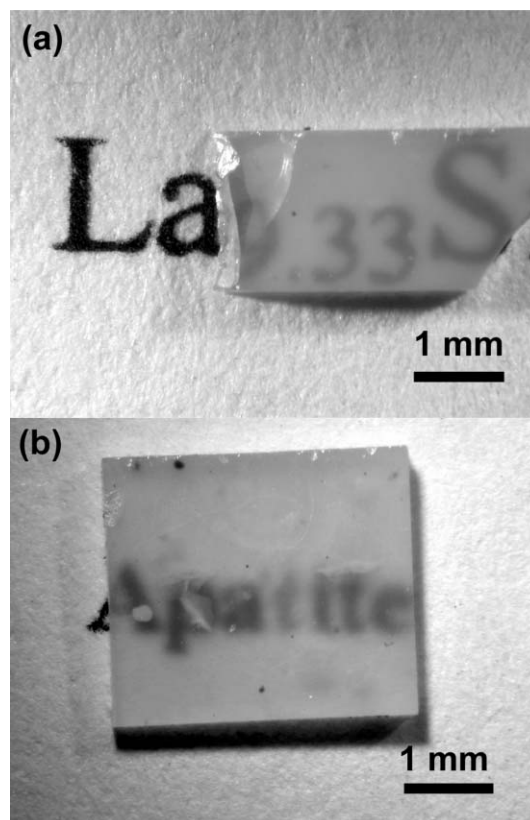


**Fig. 3** Images of the SPS-sintered ceramics, after sintering at (a) 1200 °C and (b) 1500 °C. Samples are 0.5 mm thick and were polished with SiC abrasive papers.

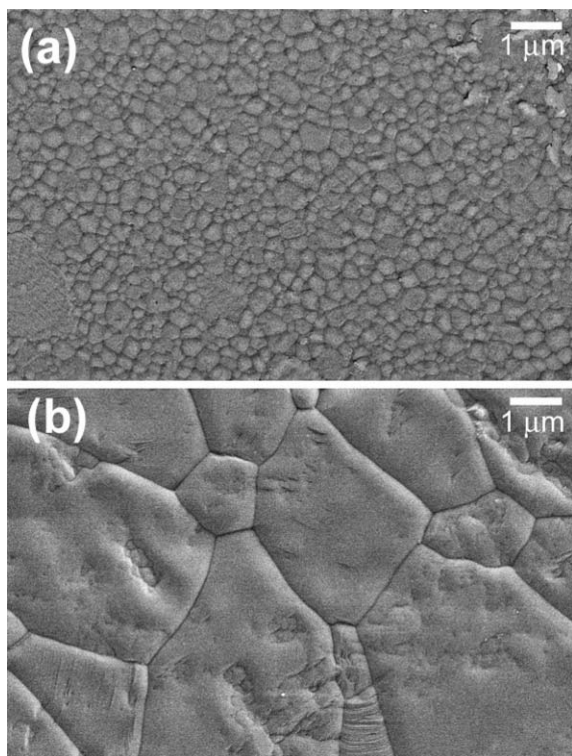


**Fig. 4** SEM images of fully dense apatite samples, SPS-sintered at (a) 1200 °C and (b) 1500 °C.

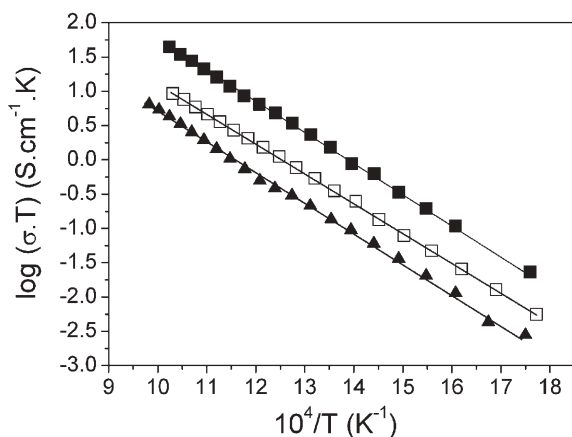


**Fig. 5** Total conductivity of  $\text{La}_{9.33}\text{Si}_6\text{O}_{26}$  samples sintered by classical sintering at 1500 °C/12 h ( $\square$ ), by spark plasma sintering at 1200 °C during 3 min ( $\blacktriangle$ ) and at 1500 °C ( $\blacksquare$ ).

Indeed, classical sintering treatments at 1500 °C/12 h with such powders lead to densities greater than 95%, which is already a very good result.

The conductivity of these samples has been evaluated by impedance spectroscopy using a solartron 1260 impedance

analyzer and a ionic-systems measurement cell. Fig. 5 shows the results of total conductivity, the most significant result for the application, although an evaluation of the bulk and grain boundary contributions could have been done at intermediate temperature. The samples present an Arrhenius like behaviour with an activation energy,  $E_a \sim 0.88(2)$  eV, similar to that previously observed.<sup>6,13</sup> The highest conductivity is obtained for the sample SPS-sintered at 1500 °C, while the lowest is obtained for the samples SPS-sintered at 1200 °C during 3 min. The sample obtained by conventional sintering shows an intermediate behaviour. The high activation energy observed plus the strong variation of conductivity with grain size suggest a significant contribution of grain boundaries in the overall conduction. Nonetheless, for the best sample, the conductivity observed is  $4.5 \times 10^{-2} \text{ S cm}^{-1}$  at 700 °C, a very good value if compared to previously reported values of  $1.1 \times 10^{-2} \text{ S cm}^{-1}$  at 700 °C for the better conducting composition  $\text{La}_{10}\text{Si}_6\text{O}_{27}$ <sup>1,2</sup> or of  $1 \times 10^{-2} \text{ S cm}^{-1}$  at 700 °C for yttria-stabilised zirconia.<sup>14</sup>

We have thus shown that a combined use of very fine and well divided powders as obtained from freeze-drying and spark plasma sintering allows to obtain very dense apatite samples, a compound known for its high resistance against densification. Such successful combination is now being extended to other hard-to-densify compounds. Among the materials tested, we are currently working on yttrium aluminium garnet (YAG) a well known laser material and on yttria-doped barium zirconate, a proton conducting compound also used in fuel cells. In this last case, the first results are promising since a density of 96% is obtained after sintering at 1600 °C during 1 min.

## Notes and references

- 1 S. Nakayama, H. Aono and Y. Sadaoka, *Chem. Lett.*, 1995, **6**, 431.
- 2 S. Nakayama and M. Sakamoto, *J. Eur. Ceram. Soc.*, 1998, **18**, 1413.
- 3 V. V. Karthon, A. L. Shaula, M. V. Patrakeev, J. C. Waernborgh, D. P. Rojas, N. P. Vyshatko, E. V. Tsipl, A. A. Yaremchenko and F. M. B. Marques, *J. Electrochem. Soc.*, 2004, **151**, A1236.
- 4 P. R. Slater, J. E. H. Sansom and J. R. Tolchard, *Chem. Rec.*, 2004, **4**, 373.
- 5 M. Yu. Gorshkov, A. D. Neumin, N. M. Bogdanovich and D. I. Bronin, *Russ. J. Electrochem.*, 2006, **42**, 737.
- 6 J. E. H. Sansom, D. Richings and P. R. Slater, *Solid State Ionics*, 2001, **139**, 205.
- 7 S. Tao and J. T. S. Irvine, *Mater. Res. Bull.*, 2001, **36**, 1245.
- 8 S. Célrier, C. Laberty, F. Ansart, P. Lenormand and P. Stevens, *Ceram. Int.*, 2006, **32**, 271.
- 9 L. Kepinski, D. Hreniak and W. Streck, *J. Alloys Compd.*, 2002, **341**, 203.
- 10 M. Yu, J. Lin and S. B. Wang, *J. Alloys Compd.*, 2002, **344**, 212.
- 11 L. Leon-Reina, E. R. Losilla, M. Martínez-Lara, S. Bruque and M. A. G. Aranda, *J. Mater. Chem.*, 2004, **14**, 1142.
- 12 H. Yoshioka and S. Tanase, *Solid State Ionics*, 2005, **176**, 2395.
- 13 A. Vincent, S. Beaudet-Savignat and F. Gervais, *J. Eur. Ceram. Soc.*, 2007, **27**, 1187.
- 14 B. C. H. Steele and A. Heinzl, *Nature*, 2001, **414**, 345.
- 15 C. J. Harlan, A. Kareiva, B. MacQueen, R. Cook and A. R. Barror, *Adv. Mater.*, 1997, **9**, 68.